Proc. Natl. Acad. Sci. USA
Vol. 91, pp. 13014–13017, December 1994
Neurobiology

Signal transmission in the parallel fiber–Purkinje cell system visualized by high-resolution imaging

(rat/brain slice/cerebellum/optical recordings/voltage-sensitive dyes)

IVO VRANESIC*, TOSHIO IIJIMA*, MICHINORI ICHIKAWA*, GEN MATSUMOTO*, AND THOMAS KNÖPFEL†‡

*Electrotechnical Laboratory, Supermolecular Science Division, 1-1-4 Umezono, Tsukuba, Ibaraki 305, Japan; and †Central Nervous System Research, K-125.6.12, Ciba, CH-4002 Basel, Switzerland

Communicated by Richard F. Thompson, September 19, 1994

ABSTRACT **We investigated the synaptic transmission in the parallel fiber–Purkinje cell system at high spatio-temporal resolution by using voltage-sensitive dyes and an imaging system. In rat cerebellar slices, cut in the frontal plane or in a plane of the cerebellar surface, local electrical stimulation induced volleys of action potentials in the parallel fibers; subsequent postsynaptic responses from Purkinje cells were observed along the volleys' entire trajectories. Furthermore, the formation of an ordered spatial gradient in parallel fiber conduction velocity across the depth of the molecular layer during postnatal development was observed. In preparations of adult, but not of immature rats, the conduction velocity of parallel fibers in the deep molecular layer was faster than in its more superficial regions. Our observations demonstrate that parallel fibers can mediate Purkinje cell excitation effectively and over considerable distances in a well-organized spatio-temporal manner, thus supporting the classical view of the physiological role assigned to the parallel fibers.**

The mossy fiber input to the cerebellar cortex is relayed via the granule cells to the Purkinje cells, each of which receives well over 100,000 excitatory synaptic inputs from granule cells. The majority of these contacts are formed with the parallel fibers—i.e., the branches of granule cell axons that run in parallel to the cerebellar surface. A smaller number of synaptic contacts are formed with the vertically ascending portions of the granule cell axons before they bifurcate and give rise to the actual parallel fibers (1, 2). The classical view of the functional organization of the cerebellar cortex is based on the effectiveness of signal transmission at the parallel fiber–Purkinje cell synapses (3–10) along activated beams of parallel fibers. The pivotal role of signal transmission at these synapses has been questioned, based on the argument that the strongest and best synchronized synaptic input to the Purkinje cells is provided by the synapses formed with the ascending granule cell axons (2, 11, 12). In this picture, local mossy fiber inputs are processed by the Purkinje cells in the immediate neighborhood of that input. By using voltage-sensitive dyes (13, 14) and an optical recording system (15), we imaged the spread of action potential volleys in the parallel fibers. Subsequent postsynaptic responses from Purkinje cells were observed along the volleys' entire trajectories. In preparations of adult rats, the conduction velocity of parallel fibers in the deep molecular layer was faster than in its more superficial regions. Our observations demonstrate that parallel fibers can mediate Purkinje cell excitation effectively and over considerable distances in a well-organized spatio-temporal manner whose characteristics are adjusted during postnatal development. Our observations support the classical view of the physiological role assigned to the parallel fibers (3–10).

The publication costs of this article were defrayed in part by page charge payment. This article must therefore be hereby marked "*advertisement*" in accordance with 18 U.S.C. §1734 solely to indicate this fact.

MATERIALS AND METHODS

Cerebellar Slices and Recording Setup. Wistar rats (either sex, aged between 16 days and 5 weeks) were anesthetized by exposure to diethyl ether and then decapitated. Slices were cut from the cerebellar vermis in parafrontal planes ("frontal" slices, 200 μm) or in parallel to the cerebellar surface ("superficial" slices, 400 μm) with a Vibroslice (Campden Instruments) and left to recover for 30–60 min at 32°C in continuously oxygenated (95% O_2/5% CO_2) artificial cerebrospinal fluid (ACSF, 147 mm Na^+/5 mM K^+/2 mM Ca^{2+}/2 mM Mg^{2+}/133 mM Cl^-/ 1 mM $H_2PO_4^-$/22 mM HCO_3^-/2 mM SO_4^{2-}/10 mM D-glucose. For experiments, slices were transferred to a recording chamber attached to the stage of an upright microscope (Zeiss Axioplan) and superfused with continuously oxygenated ACSF (32°C). Electrical stimuli (current pulses of 1.0–2.5 mA, applied for 200–600 μs) were delivered to the tissue with bipolar stimulation electrodes (tip spacing, 100–200 μm) placed in the molecular layer of the frontal slices or on the pial surface of the superficial preparations.

Optical Recordings of Local Membrane Potential Changes. Preparations were stained in the recording chamber with the voltage-sensitive absorbance dye RH-155 (2 mM dissolved in ACSF; see refs. 13 and 14). For transmission microphotometry of membrane-potential-dependent absorbance changes, preparations were illuminated with a tungsten lamp. A shutter in the light path was used to restrict exposure of the stained preparations to the light to the time of actual recordings (150 ms) to minimize the photo-induced toxic effects and bleaching of the dye. Transmitted light was passed through an interference band pass filter (720 ± 15 nm) and projected onto the low-noise imaging system (64 × 64 pixels; internal 12-bit representation; frame rate, 1.7 kHz; see ref. 15). All illustrated imaging data represent the average of 32 sweeps obtained in intervals of 2 s.

Determination of Propagation Velocities. To determine the propagation velocity of action potentials along the parallel fibers, the latency between optical signal peak and stimulus delivery was measured at equidistantly spaced points (between 20 and 70 pixels) along the direction of propagation (e.g., see Fig. 3*B*). The propagation velocity was then assessed with linear regression analysis (the linear correlation coefficients were better than 0.97 in 50% of all cases). Velocity profiles across the depth of the molecular layer were obtained by determining signal propagation velocities along equidistantly spaced lines (usually by one pixel width) covering the responsive area of the molecular layer. Data analysis and reproduction were performed with a UNIX-based software package.

RESULTS

Parallel Fiber Volleys Mediate Purkinje Cell Excitation Over Long Distances. We used voltage-sensitive dyes (13, 14) and

Abbreviation: ACSF, artificial cerebrospinal fluid.

‡To whom reprint requests should be addressed.

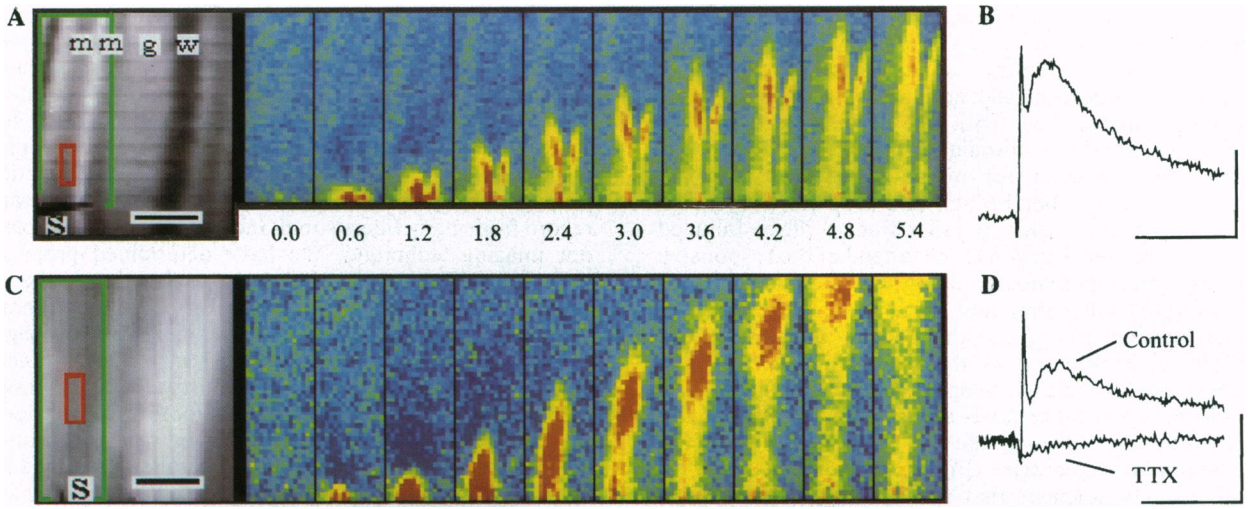

FIG. 1. Spread of electrical activity as detected with a voltage-sensitive dye in frontal (*A* and *B*) and superficial (*C* and *D*) slices of rat cerebellar cortex. (*A Left*), Transmission microphotograph of a frontal preparation of a 19-day-old rat. Indicated are the locations of the stimulation electrode (S), white matter (w), granule cell layer (g), and two adjacent molecular layers (m). (Bar = 400 μm.) (*Right*) Color-coded imaging sequence of optical signals in the molecular layer taken from the region indicated by green rectangle. Blue colors correspond to resting membrane potential; yellow through red colors correspond to membrane depolarization. Individual frames were acquired at time points given below (in ms, relative to stimulus delivery). (*B*) Time course of optical signals obtained from region indicated by red rectangle in *A*. Vertical and horizontal scale bars indicate 0.1% fractional absorbance change and 50 ms. (*C Left*) Transmission microphotograph of a superficial preparation of a 20-day-old rat. (Bar = 200 μm). Location of stimulation electrode is marked by s. (*Right*) Color-coded imaging sequence analogous to *A* with the same stimulation parameters and time marks. (*D*) Time course of optical signals under control conditions and after addition of 1 μM tetrodotoxin (TTX) to the perfusate. Vertical and horizontal calibration bars indicate 0.05% fractional absorbance change and 50 ms, respectively.

an imaging system (15) to optically record neuronal activity in two types of rat cerebellar slices. In slices cut in the frontal plane, electrical stimulation of the molecular layer induced a biphasic optical signal that spread along the parallel fibers. The signals were due to membrane depolarization (13, 14) and consisted of an initial fast spike-like component and a subsequent slower component (Fig. 1 *A* and *B*). Corresponding recordings were obtained from slices cut in parallel to the cerebellar surface (Fig. 1 *C* and *D*). There, electrical stimuli applied to the pial surface of the preparations gave rise to depolarizing voltage signals that spread in beam-like structures along the parallel fibers (16, 17). All signals were abolished in 1 μM tetrodotoxin (n = 3; Fig. 1*D*); the late component was strongly and reversibly depressed in nominally calcium-free medium (n = 5, Fig. 2*A*). We therefore identified the initial fast signals as presynaptic action potentials that propagate along the parallel fibers and the following signals as excitatory postsynaptic responses (16). The bulk of these postsynaptic responses arises from Purkinje cells because (*i*) their dendritic arborization constitutes the largest postsynaptic membrane fraction in the molecular layer (1) and (*ii*) similar optical signals were recorded from the Purkinje cell layer where Purkinje cell bodies almost exclusively provide neuronal membranes postsynaptic to the parallel fibers. These postsynaptic responses from Purkinje cells could be generated at two qualitatively distinct sites of synaptic transmission: at the parallel fiber–Purkinje cell synapses and at the antidromically activated "ascending" synapses formed *en passant* between the ascending part of the granule cell axons and the Purkinje cells (2). In the following paragraph, we demonstrate that the dominating contribution to the observed postsynaptic responses is generated via the parallel fibers.

Relation Between Pre- and Postsynaptic Signals. Upon delivery of a focal electrical stimulus to the molecular layer of a frontal slice, the density profile of activated parallel fibers is expected to decrease monotonically (or linearly, if the parallel fibers are of equal length) with distance from the stimulation site. We assume that the density profile of parallel fiber-mediated postsynaptic responses is propor-

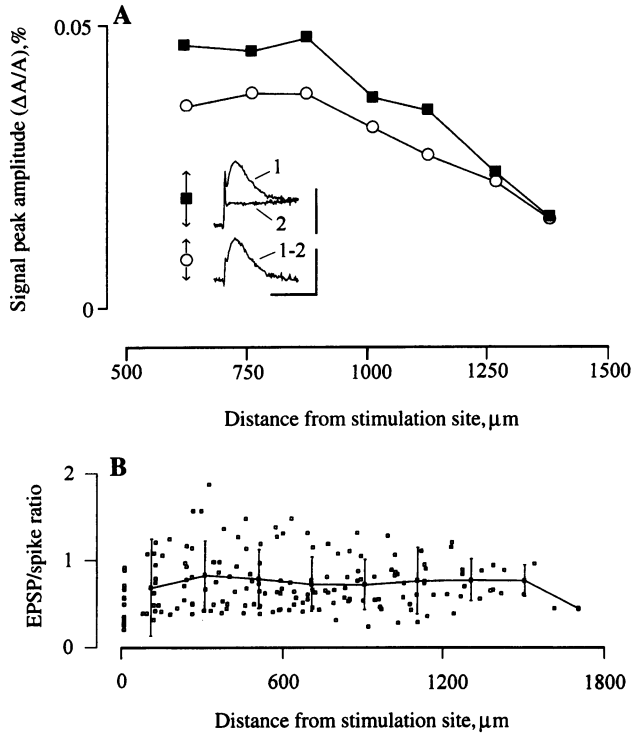

FIG. 2. Pre- and postsynaptic components of optical signals in the molecular layer of frontal and superficial preparations. (*A*) Amplitudes of parallel fiber action potentials (■) and calcium-dependent postsynaptic signals (○) plotted against distance from stimulation site along the parallel fibers. Preparation is from a 19-day-old rat. (*Inset*) Representative time courses of optical signals recorded in control solution (trace 1) and in nominally calcium-free ACSF (trace 2) and their difference (trace 1–2, calcium-dependent component). Vertical and horizontal calibration bars indicate 0.05% fractional absorbance change and 50 ms, respectively. (*B*) Amplitude ratio between post- and presynaptic components as a function of distance from stimulation site. Individual data points were obtained from eight frontal and two superficial slices; solid line connects ratios (mean ± SD) calculated after binning the pooled data into 200-μm intervals. EPSP, excitatory postsynaptic potential.

tional to the density of activated parallel fibers. In analogy, we also assume that the density of postsynaptic responses mediated via the "ascending" synapses is proportional to the density of antidromically activated ascending granule cell axons, namely, those with one of their parallel fiber branches reaching the stimulation site. This density is approximately constant for distances shorter than the length of a parallel fiber branch and zero for longer distances. We observed that parallel fiber volleys induced postsynaptic responses even at the far end of the responsive molecular layer, where no ascending synapses are expected to be activated antidromically (Fig. 2*A*). The density of activated parallel fibers and the density of postsynaptic potentials were assessed as the peak amplitudes of the initial fast and the late slow optical signals, respectively. The ratio between these post- and presynaptic signal amplitudes was constant over the full range of the observed action potential trajectories (Fig. 2*B*). This constant proportion strongly suggests that parallel fibers can mediate postsynaptic responses over their entire length and thus drive the Purkinje cells over appreciable distances. Were the observed postsynaptic responses mediated exclusively by antidromic activation of ascending synapses, one would expect the signal amplitude ratio to increase to roughly twice its initial value by a distance equal to the length of a parallel fiber branch and decline rapidly to zero for longer distances.

Spatial Distribution of Parallel Fiber Conduction Velocity Across the Depth of the Molecular Layer. The conduction velocity of the parallel fibers is a critical parameter in several proposals on the function of the cerebellar cortex. It has been argued that a slow and spatially well-organized conduction velocity enables the parallel fiber–Purkinje cell system to decode temporal patterns of mossy fiber activity (8–10). In an opposing view, it has been put forward that the slow and spatially inhomogeneous conduction velocity in beams of parallel fibers will result in a degradation of temporal information such that the parallel fibers would convey to the Purkinje cells a rather asynchronous signal of modulatory character (2, 11, 12). To assess the spatial organization of propagation velocity in parallel fibers, it is necessary to record from many fibers simultaneously, as was possible with our imaging technique. We have determined propagation velocity profiles at right angles to the direction of the signal propagation in preparations from 16- to 19-day-old animals and from adult rats (Fig. 3). The measured propagation velocities were between 0.2 and 0.3 m/s; these values are slightly below those reported previously (18, 19). The signals exhibited a clear discernible and smooth leading edge that marked the onset of depolarization, indicating (*i*) that there are no local inhomogeneities in the parallel fiber conduction velocity along the direction of spread and (*ii*) that the propagation velocity was similar among neighboring parallel fibers. In preparations of 19-day-old and adult animals, there was, however, a significant difference in action potential propagation velocity across the depth of the molecular layer (i.e., at right angles to the direction of action potential propagation). The spread was fastest in the deep molecular layer and slowest in its more superficial portions (Fig. 4). These observations support electron micrograph studies in rat cerebellar cortex that show that the parallel fibers in the deep molecular layer are thicker than the ones located more superficially (20) and field potential studies that suggest that parallel fiber volleys travel faster in the deeper molecular layer (21). In contrast, no significant difference in conduction velocity between superficial and deep molecular layer was

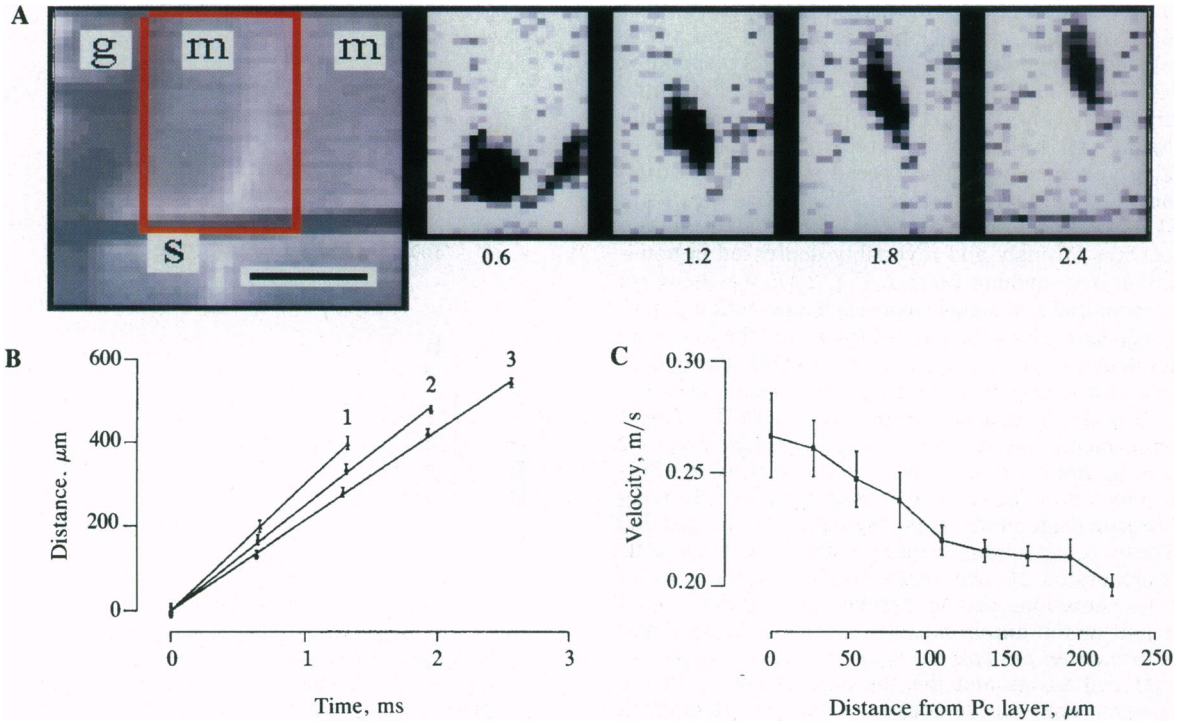

FIG. 3. Spatial variation of action propagation velocity in the parallel fibers in frontal preparations. (*A Left*) Transmission microphotograph of preparation of an adult rat. Electrical stimulus was delivered with an elongated electrode(s) that was lowered onto the tissue at right angles to the orientation of the parallel fibers. Indicated are the locations of granule cell (g) and molecular layers (m) in adjacent folia. (Bar = 400 μm.) (*Right*) Membrane potential maps extracted from region marked by red rectangle. Individual frames were acquired at time points given below (in ms, relative to stimulus delivery). Dark areas correspond to membrane depolarization. Note gradual increase in inclination of signal front; left edge is closest to Purkinje cell layer. (*B*) Determination of signal propagation velocity as slope of propagation distance vs. peak latency plots in the deep (trace 1), medial (trace 2), and superficial (trace 3) molecular layer; same preparation as in *A*. (*C*) Propagation velocity profile across the depth of the molecular layer. PC, Purkinje cell. Pial surface was at about 225 μm. Data represent mean ± SEM from six sweeps at three locations within the same preparation.

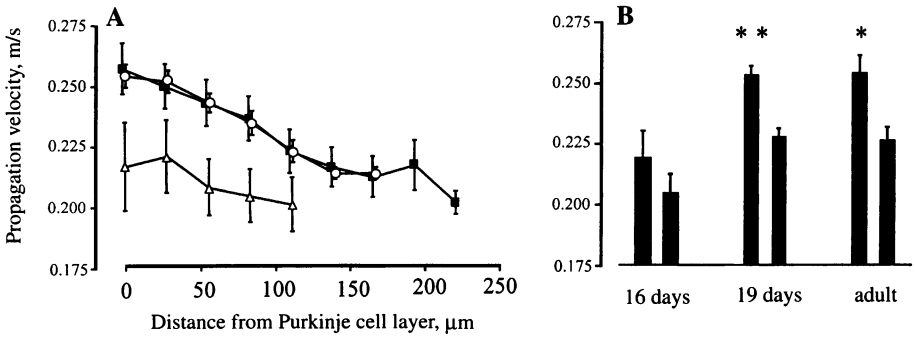

FIG. 4. Spatial distribution of action potential propagation velocities in the parallel fibers in frontal preparations. (*A*) Mean velocity profiles across the depth of the molecular layer obtained in slices of 16-day-old (Δ, $n = 5$ profiles), 19-day-old (○, $n = 19$), and adult (■, $n = 15$) rats. (*B*) Comparison of mean maximal and mean minimal propagation velocities at the respective ages. Mean maximal velocities (left bar of each pair) were determined in the deep molecular layer near the Purkinje cell layer; mean minimal propagation velocities (right bar of each pair) were determined between the medial and superficial portions of the molecular layer. In slices of 19-day-old and adult animals, the difference between mean maximal and minimal propagation velocities was statistically significant. **, $P < 1.5 \times 10^{-6}$; *, $P < 1.5 \times 10^{-3}$, respectively, by two-tailed Student's *t* test. In slices of 16-day-old animals, the difference was not significant ($P > 0.25$). The overall mean propagation velocities at 16 days, 19 days, and adulthood (two, four, and four preparations, respectively) were 0.210 ± 0.006 m/s (mean ± SEM, $n = 32$), 0.241 ± 0.002 m/s ($n = 140$), and 0.233 ± 0.004 m/s ($n = 108$).

found in the preparations of 16-day-old animals, and the mean propagation velocity was lower than in the preparations of older animals (Fig. 4). The formation of an ordered spatial gradient and the overall increase in parallel fiber conduction velocity during postnatal development provide circumstantial evidence for the notion that not only efficient transmission but also signal delays imposed in the parallel fiber pathway are of functional significance (8–10).

DISCUSSION

The present data provide decisive constraints for the validation of two conflicting views on the functional organization of the cerebellar cortex. The first view relies explicitly on the large number of functional and modifiable synapses formed between the parallel fibers and the Purkinje cells and was strongly influenced by the classical perceptron models of Marr (4) and Albus (5). The plasticity of parallel fiber–Purkinje cell synapses, as first postulated by the Marr–Albus theory, has subsequently been established (22, 23). Efficient synaptic transmission at the parallel fiber–Purkinje cell synapses is also a crucial premise for the models proposed by Braitenberg (8–10) and an adaptive filter model (6). The other view is based on the fractured somatotopic representation of the mossy fiber input on the granular layer and the congruent mapping of this representation to the Purkinje cell layer (2, 11, 12, 24). It has been argued that this vertical organization in granule cell–Purkinje cell excitatory relations reflects the major cortical information flow in the cerebellum and is mediated via the ascending synapses while lateral inputs to Purkinje cells via the parallel fibers are considered modulatory since they should lack temporal information due to the slow and inhomogeneous conduction velocity of the parallel fibers (2, 11, 12). Numerical analysis of synaptic contacts suggests that a given patch of granule cells provide roughly 10 times more ascending synapses to the patch of Purkinje cells located directly above than parallel fiber synapses to laterally displaced Purkinje cell patches of similar size (1, 2). Therefore, it is not surprising that a point-like sensory input will indeed most efficiently excite those Purkinje cells located directly above its somatotopic representation in the granule cell layer. Nonetheless, responses of Purkinje cells located outside the granule cell patch responding to a peripheral stimulus have been recently recorded in anesthetized cats (19). Furthermore, there is no reason to assume that for non-point-like (i.e., more physiological) inputs the impact of ascending fiber inputs will exceed their relative numerical weight, which amounts to about 3% of the total granule cell–Purkinje cell synaptic contacts (1, 2). Lateral patches, although each one has little effect when active alone, still provide 97% of the potential synaptic drive in the mossy fiber pathway to the Purkinje cells via the parallel fibers. Our observations indicate that the parallel fibers can relay the mossy fiber input to Purkinje cells in a well-coordinated spatio-temporal manner due to precisely adjusted conduction velocities. The present results support the view that the functional architecture of the molecular layer of the cerebellar cortex seems rather well suited for plastic (22, 23) and dynamic (6, 8–10) association between mossy fiber inputs that are represented in the granule cell layer in a spatially and temporally organized way (24).

This study was financed in part by grants from the Human Frontiers Science Program. I.V. was supported by a Science and Technology Agency Fellowship (Japan).

1. Napper, R. M. A. & Harvey, R. J. (1988) *J. Comp. Neurol.* **274**, 158–177.
2. Llinás, R. & Sugimori, M. (1992) in *The Cerebellum Revisited*, eds. Llinás, R. & Sotelo, C. (Springer, Berlin), pp. 167–181.
3. Eccles, J. C., Ito, M. & Szentagothai, J. (1967) *The Cerebellum as a Neuronal Machine* (Springer, Berlin).
4. Marr, D. (1969) *J. Physiol. (London)* **204**, 437–470.
5. Albus, J. S. (1971) *Math. Biosci.* **10**, 25–61.
6. Fujita, M. (1982) *Biol. Cybern.* **45**, 195–206.
7. It, M. (1984) *The Cerebellum and Neural Control* (Raven, New York).
8. Braitenberg, V. (1967) in *The Cerebellum*, eds. Fox, C. A. & Snider, R. S. (Elsevier, Amsterdam), pp. 334–346.
9. Braitenberg, V. (1984) *J. Theor. Neurobiol.* **2**, 237–241.
10. Braitenberg, V. (1987) in *Cerebellum and Neuronal Plasticity*, eds. Glickstein, M., Yeo, Ch. & Stein, J. (Plenum, New York), pp. 193–207.
11. Llinás, R. (1982) in *The Cerebellum New Vistas*, eds. Palay, S. L. & Chan-Palay, V. (Springer, Berlin), pp. 189–192.
12. Bower, J. M. & Woolston, D. C. (1983) *J. Neurophysiol.* **49**, 745–766.
13. Grinvald, A., Manker, A. & Segal, M. J. (1982) *J. Physiol. (London)* **333**, 269–291.
14. Grinvald, A., Frostig, R. D., Lieke, E. & Hildesheim, R. (1988) *Physiol. Rev.* **68**, 1285–1366.
15. Ichikawa, M., Iijima, T. & Matsumoto, G. (1993) in *Brain Mechanisms of Perception and Memory*, eds. Taketoshi, O., Squire, L. R., Raichle, M. E., Perret, D. I. & Fukuda, M. (Oxford Univ. Press, New York), pp. 638–648.
16. Eccles, J. C., Llinás, R. & Sasaki, K. (1966) *Exp. Brain Res.* **1**, 17–39.
17. Elias, S. A., Yac, H. & Ebner, T. J. (1993) *Neuroscience* **52**, 771–786.
18. Eccles, J. C. (1973) *J. Physiol. (London)* **229**, 1–32.
19. Garwicz, M. & Anderson, G. (1992) *Exp. Brain Res.* **88**, 615–622.
20. Fox, C. A. & Barnard, J. W. (1957) *J. Anat. (London)* **91**, 299–313.
21. Axelrad, H. & Korn, H. (1982) in *The Cerebellum New Vistas*, eds. Palay, S. L. & Chan-Palay, V. (Springer, Berlin), pp. 412–439.
22. Ito, M., Sakurai, M. & Tongroach, P. (1982) *J. Physiol. (London)* **324**, 113–134.
23. Sakurai, M. (1987) *J. Physiol. (London)* **394**, 463–480.
24. Bower, J. M., Beermann, D. H., Gibson, J. M., Shambes, G. M. & Welker, W. (1981) *Brain Behav. Evol.* **18**, 1–18.